Biomedical Physics & Engineering Express

Endorsed by IPEM Institute of Physics and Engineering in Medicine

PAPER

Application of fiber loop ringdown spectroscopy technique for a new approach to beta-amyloid monitoring for Alzheimer Disease's early detection

To cite this article: Burak Malik Kaya *et al* 2024 *Biomed. Phys. Eng. Express* **10** 035037

View the article online for updates and enhancements.

You may also like

- Study on the Amyloid A42 with Accelerated Molecular Dynamics Simulations
Kai-Fang Huang, , Shu-Heng Dong et al.
- Fiber loop ringdown gas flow sensors
Haifa Alali and Chuji Wang
- Label-free Raman and fluorescence imaging of amyloid plaques in human Alzheimer's disease brain tissue reveal carotenoid accumulations
Loes Ettema, Benjamin Lochocki, Jeroen J M Hoozemans et al.



This content was downloaded from IP address 144.122.201.61 on 06/05/2024 at 17:08

Biomedical Physics & Engineering Express

PAPER

Application of fiber loop ringdown spectroscopy technique for a new approach to beta-amyloid monitoring for Alzheimer Disease's early detection

RECEIVED
19 December 2023

REVISED
19 February 2024

ACCEPTED FOR PUBLICATION
16 April 2024

PUBLISHED
26 April 2024

Burak Malik Kaya[1,2,*], **Semih Oz**[1] and **Okan Esenturk**[3]

[1] Vocational School of Health Service, Eskisehir Osmangazi University, Eskisehir, 26480, Turkey
[2] Translational Medicine Research Center, Eskisehir Osmangazi University, Eskisehir, 26480, Turkey
[3] Department of Chemistry, Middle East Technical University, Ankara, 06800, Turkey
[*] Author to whom any correspondence should be addressed.

E-mail: malikkaya@ogu.edu.tr, semihoz@ogu.edu.tr and eokan@metu.edu.tr

Keywords: alzheimer's disease, beta-amyloid, biomarker detection, fiber optic sensors, FLRDS, local optical refractometer, biosensor

Abstract

A novel fiber optic biosensor was purposed for a new approach to monitor amyloid beta protein fragment 1–42 (Aβ42) for Alzheimer's Disease (AD) early detection. The sensor was fabricated by etching a part of fiber from single mode fiber loop in pure hydrofluoric acid solution and utilized as a Local Optical Refractometer (LOR) to monitor the change Aβ42 concentration in Artificial Cerebrospinal Fluid (ACSF). The Fiber Loop Ringdown Spectroscopy (FLRDS) technique is an ultra-sensitive measurement technique with low-cost, high sensitivity, real-time measurement, continuous measurement and portability features that was utilized with a fiber optic sensor for the first time for the detection of a biological signature in an ACSF environment. Here, the measurement is based on the total optical loss detection when specially fabricated sensor heads were immersed into ACSF solutions with and without different concentrations of Aβ42 biomarkers since the bulk refractive index change was performed. Baseline stability and the reference ring down times of the sensor head were measured in the air as 0.87% and 441.6 μs $\pm$ 3.9 μs, respectively. Afterward, the total optical loss of the system was measured when the sensor head was immersed in deionized water, ACSF solution, and ACSF solutions with Aβ42 in different concentrations. The lowest Aβ42 concentration of 2 ppm was detected by LOR. Results showed that LOR fabricated by single-mode fibers for FLRDS system design are promising candidates to be utilized as fiber optic biosensors after sensor head modification and have a high potential for early detection applications of not only AD but possibly also several fatal diseases such as diabetes and cancer.

1. Introduction

Alzheimer's Disease (AD) is a progressive neurodegenerative disease that causes irreversible damage to the brain and presents with serious deterioration in short-term memory loss, impairments of other cognitive abilities, and several psychiatric symptoms such as anxiety, stress, and depression [1, 2]. World Health Organization reported that the expense of AD treatment is approximately $600 billion because around 54 million people are affected directly or indirectly by AD. Studies emphasize that AD increases among the older population [1, 3]. AD is extremely crucial for the elder population without any treatment. Thus, continuous monitoring and the early detection of AD progresses are critically important to interfere with the disease and follow the correct therapeutic applications [3–7]. Current applications and treatments are not so effective that they are insufficient to slow down AD progress. Therefore, new approaches have significant importance to AD monitoring and early detection studies for therapeutic, diagnostic, and managing AD progression [8, 9].

Total tau (T-tau) and amyloid beta protein fragment 1–42 (Aβ42) are the best-known biomarkers for AD diagnosis, which may be tested in both cerebrospinal fluid (CSF) and serum media to differentiate with high reliability from other dementia forms

© 2024 IOP Publishing Ltd

[10, 11]. Aβ42 biomarker relevant concentration range changes between 280 and 480 pg mL^{-1} in clinical studies by utilizing traditional methods such as Enzyme-Linked Immunosorbent Assay (ELISA) [12–14]. Another study presented that CSF Aβ42 concentration changes between 200 pg ml^{-1} to 1000 pg ml^{-1} by using the Consortium to Establish a Registry for Alzheimer's Disease neuropsychological battery (CERAD-NB) testing [15]. According to the literature, a decrease in CSF-Aβ42 concentration may indicate AD early stage [13, 15]. There are several traditional techniques for Aβ42 biomarker monitoring for AD detection. Among these techniques ELISA, neuroimaging, Positron Emission Tomography (PET), and Magnetic Resonance Imaging (MRI) are conventional approaches, hence need time-consuming progress and have lower sensitivity. ELISA and neuroimaging have been the common methods to study on detection of Aβ42 and other biomarkers [16, 17]. Besides, numerous other techniques/methods have been improved for Aβ42 quantification such as fluorescent microscopy, quantum dot nanoprobes, nanomaterials, mass spectrometry, immobilized metal affinity chromatography and meta-analysis, Positron Emission Tomography (PET), Photon and Single-Photon Emission Computed Tomography, Regular and Functional Magnetic Resonance Imaging (MRI) [18–22]. Laboratory tests include genetic tests, biomarker detections, and CSF analysis [23]. In addition to aforementioned techniques, molecular imaging, mass spectrometry, and electrochemical techniques were also used for quantitative biomarker detection [24–29]. These methods and techniques have several limitations as complicated and sophisticated system design, difficulties in optimization and operation of system setup, the total cost of the systems, and challenges in obtaining high sensitivity. Among all techniques and methods, optical-based techniques have advantages in fast and direct monitoring of targets, simple system design, high sensitivity, real-time measurement, a small volume of samples, and system portability [30–35]. To overcome the aforementioned limitations, optical sensor-based methods such as optical nanosensors and surface plasmon resonance (SPR) were developed in the last decade [3, 17, 35–40]. Fiber optic-based measurement techniques allow high accuracy, fast response, low cost, simplicity, portability, specificity, and higher sensitivity [41, 42]. Even though rapid advances in technology provide some simplicity in measurement systems in these methods with higher sensitivity and target detection, there is still a need for further enhancement for suitable and convenience point-of-care (POC) diagnostics.

The evanescent field (EF) sensing mechanism combined with optical fiber sensing techniques allows high accuracy and sensitivity, repeatability, fast response, and real-time measurement. The Fiber Loop Ringdown Spectroscopy (FLRDS) technique can offer much higher sensitivity due to its multi-pass nature of the beam inside the loop, more reliable results, fast response with real-time monitoring, small size, low cost, and portability [43–45]. SPR-based fiber optic sensing techniques are performed by coating the core of fiber with a metallic layer relevant to selected biomarker detection when biomarkers interact with these films. There are few studies for AD biomarker detection by utilizing EF-fiber optic sensing mechanism. SPR technique was employed mostly by multimode fiber (MMF) [38–40] and only one with a D-shaped single-mode fiber (SMF) [46, 47]. In the SPR technique, the fiber core is coated with metallic nano-thin film, then the thin film is coated with special chemicals to detect biomarkers. Kim *et al* [38] studied fibrinogen detection in the blood plasma of AD patients utilizing MMF with the SPR technique. They covered the 5 cm sensor head region with silver (Ag) of 36 nm and aluminum (Al) of 4 nm by thermal evaporation, then 1 nm nickel (Ni) layer was coated by radio frequency magnetron sputtering technique. They set up a ring-shaped optical sensing platform and injected plasma liquid into the sensor head region to monitor the change in signal due to SPR EF penetration. They indicated the limit of detection for fibrinogen as 20 ppb. In another study, Nguyen *et al* [39] used MMF to create a sensor head and coated it with Ag, Al, and Ni layers by the same procedure as the aforementioned study. They similarly set up a ring-shaped optical sensing platform and the solution was injected into the sensor head region for the detection of fibrinogen. As a difference from the previous one, they coated the Ni layer with immunoglobulin (IgG) for the target detection of fibrinogen. They obtained the lowest detection limit of 10 ppb. Only one study with D-shaped SMF was carried on by Chiavaioli [46] for tau protein detection. He used a part of SMF to create a side-polished sensor head and coated the polished side with tin oxide (SnO_2) of 160 nm. Afterward, the sensor head was chemically modified with carboxylic groups for target sensing. They used in the system setup a multi-light emitted diode (LED) light source, optical spectrum analyzer (OSA), polarizer, and polarizer controller. After the sensor head was fabricated, it was placed into a thermally stabilized microfluid system and they obtained 5 ppm the limit of detection. Even though these studies indicate a very low limit of detection by using the advantages of measuring EF scattering/absorption, fabricated sensor heads in these techniques do not offer cylindrical symmetry which is extremely important for EF scattering/absorption measurements for more realistic results. They studied with the same sensor head design in another work [47] to perform their biosensor with IgG/anti-IgG assay by nanocoating D-shaped SMF fiber. However, the system setups used equipment and techniques are different from the one used in this study.

Nu *et al* [48] carried out their study about blood-based tau protein detection for early diagnosis of AD. They utilized a 632.8 nm He-Ne laser source, MMF

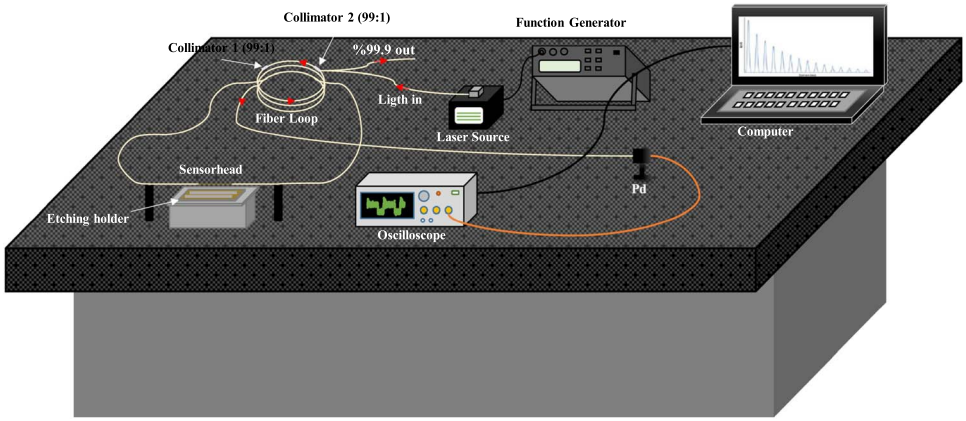


Figure 1. Fiber loop ringdown spectroscopy (FLRDS) system setup.

cable, and a photodetector. 5 cm part of MMF core was coated with 1 nm Cr and 40 nm Au metals by thermal evaporation process to produce SPR fiber sensor. Then, the He-Ne laser was coupled into the fiber which is mounted into a ring-shaped flow cell. They chemically modified the sensor surface for the target detection of tau proteins. Even though the estimated lowest detection limit was obtained for total tau and phosphorylated tau as 2.4×10^3 ppt and 1.6×10^3 ppt, respectively, the detection limit of the system is much higher than the theoretical detection limit. Kant and Gupta [49] studied an SPR fiber optic biosensor for the detection of acetylcholine for AD diagnosis. They employed a plastic fiber, unpolarised polychromatic light source, and a spectrometer to set up the system. 1 cm unclad region of fiber was coated by 40 nm silver layer with the thermal evaporation technique and then tantalum (v) oxide (Ta_2O_5) nanoparticles were deposited on the silver layer for acetylcholine detection, in which dysfunction of it linked with AD. They monitored resonance wavelength shift regarding different concentrations of acetylcholine enzyme. They tested the concentration range of 2–10 ppm and obtained a maximum shift in 6 ppm concentration. The system is composed of a single plastic fiber cable, an unpolarised polychromatic light source, and a spectrometer. Similar SPR fiber optic sensor systems were designed for the detection of various biomarkers in different solutions [37–39, 50]. All studies have their own features with disadvantages in terms of precision, ultra-high sensitivity for the early detection, portability, fast response, and immunity to electrical fluctuations. In our setup, the FLRDS system was constructed with a 1550 nm continuous wave (CW) butterfly diode laser source and its thermoelectric cooler (TEC) controller, 120 m fiber loop constructed with a single mode fiber with 99.9:0.1 couplers, 5 GHz InGaAs photodetector, an oscilloscope and computer as seen in figure 1. Fabricated Local Optical Refractometer (LOR) was directly tested for the first time in Artificial Cerebrospinal Fluid (ACSF) without Aβ42 biomarker and with Aβ42 biomarker in two different concentrations and the minimum measurable concentration was found to be 2 ppm. When they are compared with the current study, different types of fiber, system setups, and techniques were utilized in all fiber optic sensing-based studies in the literature. To the best of our knowledge, this is the first time a LOR fabricated on an SMF was applied with the FLRDS technique for the detection of Aβ42 biomarkers in ACSF solutions for the purpose of AD detection.

In this study, we demonstrate a LOR by using SMF with FLRDS technique for Aβ42 biomarker monitoring in ACSF solution by taking advantage of the Bulk Refractive Index (BRI) change-based measurement. To obtain a wide dynamic range in detection and high sensitivity of LOR, a part of fiber from the fiber loop was etched in pure hydrofluoric solution and tested in primarily deionized water (DIW) solution to exhibit LOR response in two different media; air and DIW. Afterward, LOR was used in ACSF solutions with and without Aβ42 biomarkers. We presented for the first time successive BRI change measurements due to the addition of the Aβ42 biomarker in ACSF solution fast response monitoring by utilizing the FLRDS technique. From obtained results, the current LOR integrated with the FLRDS technique can be employed as a fiber optic biosensor for future study after special modification of the surface of the sensor head for target molecule monitoring. Therefore, it has a high potential to be utilized not only for the early detection of AD, but also for several fatal diseases such as cancer, COVID-19, etc due to its outstanding features such as ultra-high sensitivity, real-time measurement, portability, low-cost, easy setup and simple design of the FLRDS system.

2. Materials and methods

2.1. The FLRDS system

The FLRDS system setup presented in figure 1 composed of two main components: the instrumentation and the sensor package. The instrumentation

consisted of a fiber-coupled CW laser diode (SFL1550S, Thorlabs, Inc. Co., New Jersey, USA) and its driver (CLD1015, Thorlabs, Inc. Co., New Jersey, USA), a photodetector (Pd) (DET08C/M) (Thorlabs, Inc. Co., New Jersey, USA), and electronic equipment to control the system. A function generator was used to convert sinusoidal wave to square wave. An oscilloscope (1202B, Tektronix Inc., Leeds, United Kingdom) with 200 MHz bandwidth was utilized to monitor the intensity decay curve. The FLRDS loop constituted from a 120 m single-mode fiber (SMF) loop (SMF28e, Corning Inc., Corning, NY, USA) of two identical 99.9:0.1 couplers (Opneti Communication Co., Shenzhen, China) and the created sensor head by etching with hydrofluoric acid (48% purity, #100334 Merck, Darmstadt, Germany) a part of fiber from the fiber loop. The etched fiber length to create a sensor head is 5 cm long. The length of the fiber loop in any FLRDS system must tolerate a laser pulse for a complete single turn inside the loop. Otherwise, ringdowns of consecutive pulses will overlap and observation of the ringdown event becomes difficult. The system properties were given in detail in [51].

Figure 1 was setup in our Optics & Photonics laboratory in Eskisehir Osmangazi University by utilizing aforementioned components for the purpose of detection and monitoring by the evanescent field (EF) change of the utilized light pulse in the fiber loop. The rationale of the setup in figure 1 is to enhance turning number of trapped laser pulse in the fiber loop until it decays to increase interaction of the laser pulse with measured samples. The FLRDS system optimization is extremely important for the setup evaluation in terms of the system stability, lowest detection limit, repeatability and sensitivity. The system sensitivity is the most important one among them so that it is calculated by collecting consecutive several data and calculating the baseline stability and the signal-to-noise (S/N) ratio of the system. The more the interaction between the light pulse and the measurands occurs in the sensor region, the higher sensitivity and the more reliable results can be obtained. The EF changes depends on the refractive index of the sensor region environment. Thus, very small changes can be detectable if only the FLRDS system optimization is well-aligned. When the sensorhead was chemically modified and coated with special chemicals, the FLRDS system could be utilized for target molecule sensing purpose.

The diameters of the core (8.2 μm) and the cladding (125 μm) of SMF was used in these study. The optical loss in total, including absorption loss, insertion losses and the losses in the couplers, while the laser beam propagates in the loop, was obtained to be less than 0.40 dB.

A 5 cm long fiber region was chosen as the sensor head region. To create the sensor head, first; 5 cm part from the fiber loop was selected, second; the plastic jacket of this part was removed, and third; this part was chemically etched in hydrofluoric (HF, 48%) acid solution for approximately 75 min. HF solution was in the solution holder so that it was placed on the lab jack which can move up and down easily. The system optic loss was increased when the cladding diameter was reduced by etching progress. After the best sensor head with higher sensitivity was fabricated, it was tested in DIW and air several times and becomes ready to be used in measurements. The best sensitivity was obtained when the fiber diameter in the sensor region is reduced to 35 ± 5 μm thickness. Details on the procedure are given in [51–58]. The optimized system performance for the best signal-to-noise (S/N), where laser current, working temperature, driver temperature, and thermoelectric cooler current were carefully adjusted and optimized. For the optimization, the laser diode current, laser working temperature, driver temperature, and current of the thermoelectric cooler (TEC) were precisely adjusted to obtain the lowest S/N ratio. The system was optimized by keeping TEC current and temperature as clarified in the instruction manual and changing the laser diode current and working temperature between 270–350 mA with 1 mA steps and 30 °C–45 °C with 1 °C steps, respectively. The best S/N ratio was obtained at 297 mA laser current and 38 °C working temperature. In this work, the S/N ratio was calculated by using the average ringdown time (RDT) and the standard deviation of the data.

ACSF (Tocris Bioscience, #3525, Bristol, United Kingdom) and Aβ42 (Merck, #A9810 Darmstadt, Germany) were commercially purchased. For the dissolution and storage process of Aβ42, 4 mM Dimethyl Sulfoxide (DMSO) (CAS 67-68-5, Merck) solution was prepared in 1 L DIW as shown in figure 2, as follows: First, 1 mg Aβ42 was added into 1 mL solution of previously prepared 4 mM DMSO solution. Second, it was separated into 150 μL aliquots and kept at −20 °C. Test solutions were separately prepared with 10 μL and 20 μL Aβ42 concentrations in 5 mL ACSF solutions. DIW and ACSF with and without Aβ42 test solutions were filled into a sampling compartment (solution holder in figure 1) in equal volumes. Then, measurements were carried out by immersing 5 cm sensor head into the solution and exposing it to air repeatedly at which system RDTs were recorded for both cases. In this work, the detection of Aβ42 concentration in ACSF was performed by monitoring the RDT changes while keeping all other variables constant. DIW was used as a control measurement to represent the sensor system RDT response difference from the ACSF solution. RDT measurement of ACSF solution without Aβ42 is our reference measurement. Following, Aβ42 was added to the ACSF solution in different concentrations, and RDTs were recorded. Thus, the effect of Aβ42 amounts on the system's total optical loss was measured by monitoring the changes in RDT values.

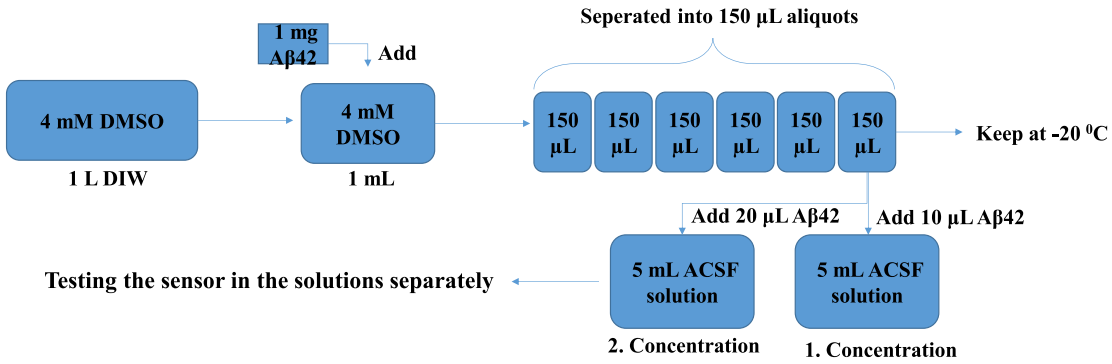


Figure 2. Schematic diagram of preparation of the testing solutions.

2.2. The FLRDS system

The coupled light beam inside the fiber loop travels several round trips until it dies out. The light beam intensity decreases with each single turn due to decreasing optical loss and hence the signals the photodetector collects will be tend to exponentially decreasing. The intensity of collected signals (I) by the photodetector is given by [51–53]

$$I = I_0 e^{(Act/nL)} \tag{1}$$

where I_0 is incident beam intensity, A is the total fiber transmission loss of the beam per round trip, c is the speed of light, t is the decay time, n is the average refractive index and L is the total length of the fiber loop. The time taken to decrease I to I_o/e is referred to as ringdown time (RDT), τ_0, of the reference system and is written by equation (2).

$$\tau_0 = \frac{nL}{cA}. \tag{2}$$

$$\tau = \frac{nL}{c(A + B)}. \tag{3}$$

Equation (3) presents the system with additional losses, B, when, for example, medium changes around the sensor head. Here in equations (2) and (3), the average refractive index (RI) of the fiber is considered to be constant given very small region of fiber being immersed compared to the loop. The effect of external pressure on the average RI of fiber, as discussed in [59, 60], can be negligible because in our study, pressure due to liquid on the sensor head was extremely low and there was no other additional pressure. For an FLRDS system, the total transmission loss is determined by the FLRD parameters such as absorption loss of fiber, insertion losses in the couplers and transmission loss. However, once a sensing action happens on the sensor head such as medium change around the sensor head, an additional optical loss, B, is created. RDT (τ) change because of created extra optical loss is given by equation (4), derived from equations (2) and (3)

$$B = \frac{nL}{c}\left(\frac{1}{\tau}\frac{1}{\tau_0}\right). \tag{4}$$

Thus, this system can be used as a sensitive chemical or biochemical sensor, or a LOR. For this kind of FLRDS chemical LOR, B denotes the optical loss differences between the reference and the sample, such as air and water. Since water and air have different refractive indexes, optical losses change and RDT will be affected whenever the sensor head is immersed in the water solution. Assuming there is no loss associated with absorption, the amount of evanescent field (EF) loss will be different in different refractive indices. Thus, recorded RDTs between air and water are different [53–55].

The lowest measurable optical loss can be obtained by equation (5):

$$B_{min} = \frac{t_r}{\tau_0}\left(\frac{\sigma}{\tau_{ave}}\right) = \frac{1}{m}\frac{\sigma}{\tau_{ave}} \tag{5}$$

where t_r is the round trip time of the laser beam in the loop, m is the number of rounds, and σ is the standard deviation. σ/τ_{ave} is the stability of the baseline. The minimum measurable RDT ($\tau_{\min}$) is obtained as 3.84 μs by using the baseline stability and sensor RDT without any action on the sensor head. In this work, theoretical t_r and τ_0 are calculated as 587.5 ns and 7.19 μs for 120 m loop, respectively. This corresponds to a *m value of* 12. Further details on baseline stability calculations can be found in [51, 57, 58].

The cross-sensitivity issue is well-defined in [61, 62] and is directly related to biosensor specificity. In this study, the detection of Aβ42 in ACSF solution was performed based on BRI change measurement which is explained in [56, 62] in detail. On the contrary to the surface refractive index (SRI) change-based measurement, BRI change-based measurements offer more advantages such as higher sensitivity and minimum affect from bending events [62]. Therefore, it was considered that the evanescent field change on the sensor head region is mostly attributed to the BRI change. Hence, BRI-based Aβ42 biomarker detection was carried out with continuous monitoring in this study. The bending effect around the sensor head was

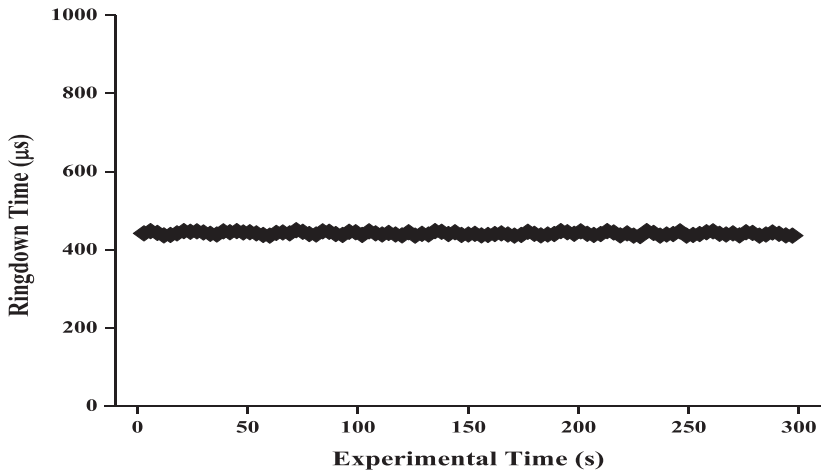


Figure 3. Baseline stability of FLRDS LOR system.

minimized by stretching the sensorhead region using two identical supports before starting the experiment as shown in figure 4(b).

Several strengths such as fast response, high sensitivity, real-time monitoring and allowing to be a portable measurement system of the FLRDS technique highlighted this study as a new measurement system for biomarkers in different diseases such as AD. Target molecule sensing and relatively higher baseline can be attributed for this study as the limitations. To enhance the baseline stability, sensing system components must be upgraded with a diligent optimization such as a better light source, a power supply for the constant electrical power, a high frequency range oscilloscope and photodetector. For the target molecule sensing process, the sensorhead must be chemically modified and coated with special chemicals so that the main target in our next project.

3. Results and discussions

Figure 3 shows the baseline stability of the FLRDS LOR system using the 5 cm sensor head. Here, data were recorded in air and there are no external effects on the sensor head such as pressure, bending, or strain. The RDT, standard deviation, and baseline stability were calculated from a hundred data collected in an air medium where each data is an average of 128 readings. The average RDT was measured as 441.6 $\pm$ 3.9 μs and the baseline stability of the system was calculated as 0.87%.

Figure 4(a) presents RDT measurements with LOR in two different media; air and DIW solution. The measurement was repeated seven times alternating between air and DIW to show the LOR integrated sensor system can supply repeatable data. RDT values with the LOR were recorded as 402.4 μs and 451.3 μs for air and DIW solution, respectively. Reported RDT values in air presented in figure 3 and figure 4(a) are different because the sensor head region was slightly bent from two points as seen in figure 4(b) (highlighted region) to avoid both floating of the sensor head in solutions and to minimize the vibration effect. The change in the total optical loss of the system when the sensor head was immersed in DIW solution from an air medium was calculated as 160 μdB. Measurable minimum optical loss with this kind of FLRDS system was calculated by using equation (5) as 11 μdB.

Figure 5 shows RDT measurements with LOR in air, DIW, and ACSF solutions. The RDT of the air further decreased to 346.4 μs because of an accidental extra bending that occurred while adjusting the sensor region for the new measurements. The RDT of the system changed in this data set due to the bending/pressure of the sensor head region on the support points in figure 4(b). The RDT of the system was first recorded in the air. Following, the sensor head was immersed in DIW solution and then exposed to air. The RDT value was recorded as 370.1 μs when the sensor head was immersed in DIW solutions. Later, RDT measurements in ACSF solutions were repeated several times. The RDT value was changed to 376.3 μs as soon as the sensor head was immersed into the ACSF solution. Finally, the sensor head was tested in DIW solution to show that the sensor can read repeatable results. The difference observed in the RDT values of the DIW and the ACSF solution is mainly due to the differences in their refractive indexes (RIs). RIs of ACSF and DIW solutions are 1.342 and 1.333, respectively [50, 63]. The system optical loss difference when the sensor head was immersed into DIW and ACSF solutions was calculated as 25 μdB, which is higher than the detectible minimum optical loss. The results show that the FLRDS LOR can differentiate these two solutions.

Figure 6 presents RDT measurements with LOR in DIW and two different ACSF solutions having 1:500 (v/v) (2 ppm) and 1:250 (v/v) (4 ppm) Aβ42 biomarker concentrations. Here, Aβ42 biomarker sample solutions were prepared by using DMSO as stated in the materials part. First, the sensor reading was

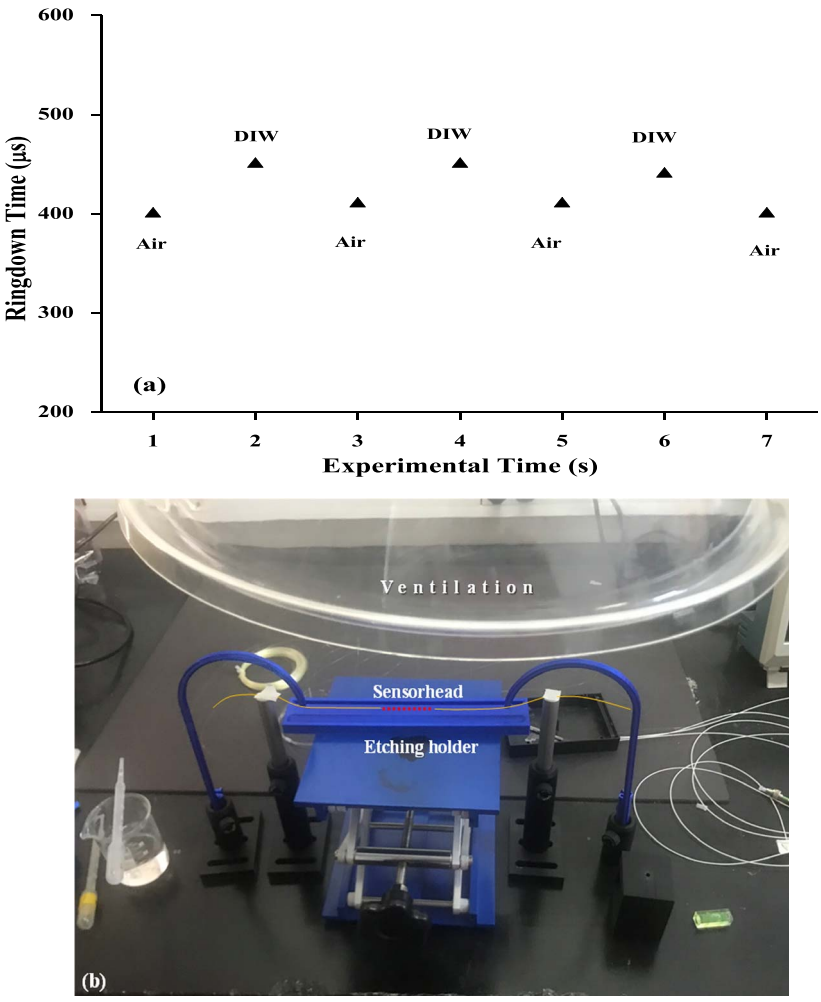


Figure 4. (a) Air-DIW tests of LOR and (b) the sensor head region design.

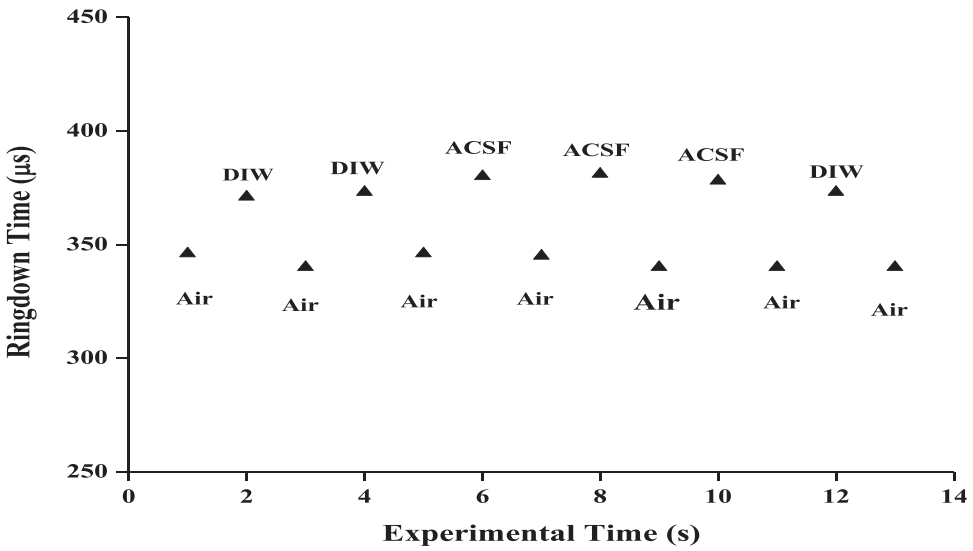


Figure 5. Tests of LOR in ACSF solution.

completed in air and then in DIW solution as reference readings. The resulting RDT values are 341.2 μs and 373.5 μs, respectively. Following, the sensor region was exposed to air again and RDT was measured and then immersed into 2 ppm Aβ42 solution. The recorded RDT in the solution mixture was 384.7 μs. The change is highly significant. Later, the sensor head was exposed to air again and then

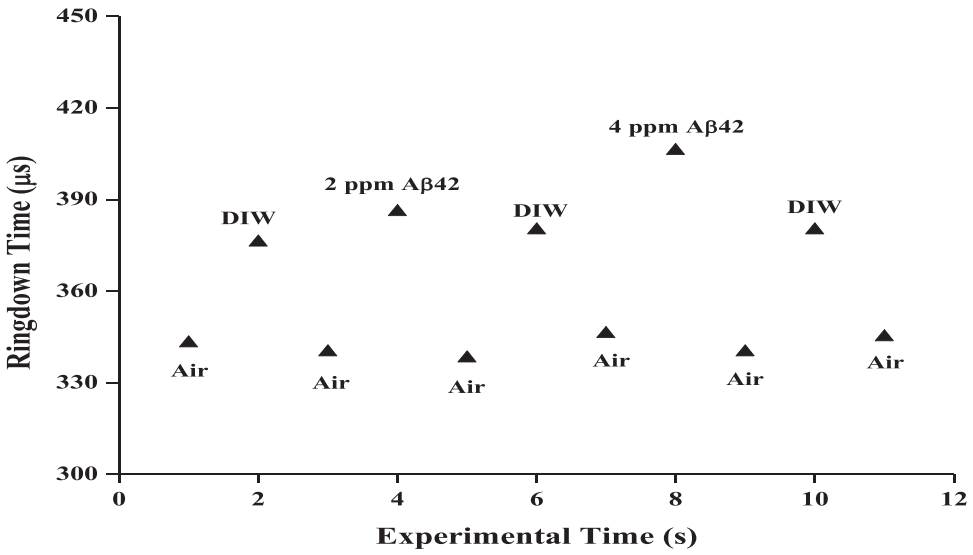


Figure 6. Tests of LOR in different Aβ42 concentrations.

immersed in 4 ppm Aβ42 solution. RDT was significantly increased as expected to a value of 404.1 μs. Since the measured Aβ42 concentration in ACSF was on ppm levels, the chance in RDT was observed. As mentioned before, any change in RDT indicates a change in the total optical loss of the system. If the change is positive, hence a decrease in RDT, this means an increase in total optical losses, either as increased absorption or due to a change in refractive index. If the change is negative, hence an increase in RDT, that means a decrease in total optical losses. Thus, increasing RDT reveals decreasing optical loss as the concentration of Aβ42 is increased in solution. The system total optical loss changed when the sensor head was immersed into DIW and then 2 ppm Aβ42 solution is calculated as 45 μdB, which is much higher than the minimum detectable optical loss of the system. Following, the sensor head was exposed to air and then immersed in DIW solution. The RDTs were decreased to initial values for both air and DIW media. Then the sensor head was immersed in 4 ppm Aβ42 solution. The change in the total optical loss of the system when the sensor head was in 2 ppm and 4 ppm Aβ42 solutions was calculated as 75 μdB. Here the observed increase in RDTs of Aβ42-ACSF solutions was associated with the changes in their refractive indexes. The FLRDS LOR fabricated in the laboratory conditions was employed for the purpose of early detection in AD by monitoring of the system RDT change with changing Aβ42 biomarker concentration by BRI change-based measurement.

There are numerous studies on Aβ42 biomarker monitoring for AD detection. Even though the FLRDS technique is not a new technique itself, it was applied for Aβ42 detection in ACSF solution for the first time by using BRI change measurement. All studies have their own features with advantages/disadvantages in terms of system design, cost, precision, sensitivity for early detection, portability, fast response, and immunity to electrical fluctuations. Kant and Gupta [49] studied SPR fiber optic biosensor for the detection of acetylcholine for AD diagnosis. They monitored resonance wavelength shift regarding different concentrations of acetylcholine enzyme. They tested the concentration range of 2–10 ppm and obtained a maximum shift in 6 ppm concentration. Their system is different from the FLRDS system and composed of a single plastic fiber cable, an unpolarised polychromatic light source, and a spectrometer. Similar SPR fiber optic sensor systems were designed for the detection of various biomarkers in different solutions [37–39, 64]. Sun *et al* [50] studied the optical coherence tomography (OCT) system to measure regional RIs in acute brain tissue slices. They detected RIs by measuring by dividing optical thickness by the physical thickness of tissue slices. Their system design and used measurement technique are different from our study in terms of used technique, system equipment, and design. In our study, used technique and system setup studies are different from all studies focused on Aβ42 biomarker detection. In our setup, the FLRDS system allows simplicity, portability, insensitivity to electrical fluctuations, fast response, and continuous monitoring. The results obtained in this study are comparable with the aforementioned studies. FLRDS system must be further enhanced by replacing the laser source with very narrow laser pulses, high sensitive detector, and an oscilloscope with higher bandwidth capability for lower sensing limits in ppb levels. The theoretical limit can be further enhanced by using a pulsed laser as a light source with a stabilized system to decrease background noise in the FLRDS system. Outstanding features of the FLRDS technique can yield an early diagnosis of crucial diseases such as cancer, AD, diabetes, etc The results suggest that the FLRDS system offers ultra-high sensitivity due to the interaction of

trapped laser pulse inside the fiber loop with measurands. Therefore, the FLRDS technique offers more precise results, real-time monitoring with fast response, ultra-high sensitivity, portability, small size, and simple setup when it is compared with its counterparts. For future study, the sensor head will be chemically modified to produce fiber optic biosensors with antibodies of special target molecules for target molecule sensing. Employing the fascinating nature of the FLRDS technique with fiber optic sensors (FOS), they have a wide range of application areas in medicine, biomedical, structural health monitoring, chemical trace element, and detecting physical parameters.

4. Conclusion

A new type of LOR was fabricated and employed for the first time with an ultra-high sensitive sensing technique, FLRDS, to observe the Aβ42 biomarker in ACSF for the early detection of Alzheimer's Diseases. The biomarker solutions were prepared by first dissolving 1 mg Aβ42 in 1 mL dimethyl sulfoxide (DMSO). Next, volume-by-volume concentrations of Aβ42 in ACSF were obtained at two different concentrations; 2 ppm and 4 ppm. The baseline stability and the minimum detectable optical loss of the LOR-integrated FLRDS system were obtained to be 0.87% and 11 μdB, respectively. Afterward, the RDTs of the LOR FLRDS were measured in air and DIW to show the repeated data. Following, the sensors were used to measure RDTs in ACSF solutions without and with Aβ42 biomarker concentrations of 2 ppm and 4 ppm, respectively. The presented system offers several outstanding advantages such as fast response ($<$ 1 s), low-cost system design, portability, small size, and simple setup. The FLRDS LOR system sensitivity and selectivity can be further enhanced both by increasing the interaction time of a trapped laser beam inside the fiber loop with measurands and by modification of the sensor head by a special chemical process for the target molecule sensing. Hence, such an FLRDS LOR system can be utilized in numerous applications such as biomedical, medicine, structural health monitoring, chemical trace elements, physical sensors, etc Therefore, these systems have high potential due to its merits in sensitivity, system total cost, portability, small volume, fast response with real-time monitoring, and immunity to electrical interference.

Data availability statement

All data that support the findings of this study are included within the article (and any supplementary files).

Author contributions

BMK contributed to the study conception and design. Material preparation, data collection and analysis were performed by BMK and OE. First draft and draft revision of the manuscript were prepared by BMK, SO, and OE. All authors commented on previous versions of the manuscript. All authors read and approved the final manuscript.

Funding

This paper is based upon work supported by Eskisehir Osmangazi University BAP project under 201841074 project code, Turkey.

Conflicts of interest

The authors declare no conflict of interest. The funders had no role in the design of the study; in the collection, analyses, or interpretation of the data; in the writing of the manuscript, or in the decision to publish the results.

ORCID iDs

Burak Malik Kaya https://orcid.org/0000-0002-1251-6915
Semih Oz https://orcid.org/0000-0002-1543-2223
Okan Esenturk https://orcid.org/0000-0001-6539-4344

References

[1] Mount C and Downton C 2006 Alzheimer disease: progress or profit? *Nat. Med.* **12** 780–4
[2] Claeysen S, Bockaert J and Giannoni P 2015 Serotonin: a new hope in Alzheimer's Disease? *ACS Chem. Neurosci.* **7** 940–3
[3] Kaushik A, Jayant R D, Tiwari S, Vashist A and Nair M 2016 Nano-biosensors to detect beta-amyloid for Alzheimer's Disease management *Biosens. Bioelectron.* **80** 273–87
[4] Piau A, Wild K, Mattek N and Kaye J 2019 Current state of digital biomarker technologies for real-life, home-based monitoring of cognitive function for mild cognitive impairment to mild Alzheimer Disease and implications for clinical care: systematic review *J Med Internet Res* **21** 1–26
[5] Masconi L, Berti V, Glodzik L, Santi S D and De Leon M J 2010 Pre-clinical detection of Alzheimer's Disease using FDG-PET, with or without amyloid imaging *J Alzheimer's Dis* **20** 843–54
[6] Haes A J, Chang L, Klein W L and Duyne R P V 2005 Detection of a biomarker for Alzheimer's Disease from synthetic and clinical samples using a nanoscale optical biosensor *J. Am. Chem. Soc.* **7** 2264–71
[7] Rushword J V, Ahmed A, Griffiths H H, Pollock N M, Hooper N M and Millner P A 2014 A label-free electrical impedimetric biosensor for the specific detection of Alzheimer's amyloid-beta oligomers *Biosens. Bioelectron.* **56** 83–90
[8] Laske C *et al* 2015 Innovative diagnostic tools for early detection of Alzheimer's Disease *Alzheimers Dement* **11** 561–78
[9] Mosconi L, Brys M, Sobanska L G, De Santi S, Rusinek H and De Leon J M 2007 Early detection of Alzheimer's Disease using neuroimaging *Exp. Gerontol.* **42** 129–38

[10] Albert M S *et al* 2011 The diagnosis of mild cognitive impairment due to Alzheimer's Disease: recommendations from the National Institute on Aging-Alzheimer's Association workgroups on diagnostic guidelines for Alzheimer's Disease *Alzheimers Dement* **7** 270–9
[11] Mulder C, Verwey N A, Van der Flier W M, Bouwman F H, Kok A, van Elk E J, Schelten P and Blankestein M A 2010 Amyloid-β(1–42), total tau, and phosphorylated tau as cerebrospinal fluid biomarkers for the diagnosis of Alzheimer Disease *Clin. Chem.* **56** 248–53
[12] Song C, Deng P and Que L 2018 Rapid multiplexed detection of beta-amyloid and total-tau as biomarkers for Alzheimer's Disease in cerebrospinal fluid *Nanomed. Nanotechnol. Biol. Med.* **14** 1845–52
[13] Hampel H and Blennow K 2004 CSF tau and β-amyloid as biomarkers for mild cognitive impairment *Dialogues Clin. Neurosci.* **6** 379–90
[14] Mo J A, Lim J H, Sul A R, Lee M, Youn Y C and Kim H J 2015 Cerebrospinal fluid β-Amyloid1–42 levels in the differential diagnosis of Alzheimer's disease-systematic review and meta-analysis *PLoS One* **10** e0116802
[15] Haapalinna F *et al* 2016 Low cerebrospinal fluid amyloid-beta concentration is associated with poorer delayed memory recall in women *Dement Ger Cogn Disorders Extra* **6** 303–12
[16] Song L, Lachno D R, Hanlon D, Shepro A, Jeromin A, Gemani D, Talbot J A, Racke M M, Dage J L and Dean R A 2016 A digital enzyme-linked immunosorbent assay for ultrasensitive measurement of amyloid-β1–42 peptide in human plasma with utility for studies of Alzheimer's Disease therapeutics *Alzheimer's Res Ther* **8** 58–65
[17] Kang J H, Vanderstichele H, Trojanowski J Q and Shaw L M 2012 Simultaneous analysis of cerebrospinal fluid biomarkers using microsphere-based xMAP multiplex technology for early detection of Alzheimer's Disease *Methods* **56** 484–93
[18] Zhao J, Ding X, Du Y, Wang X and Men G 2019 Functional connectivity between white matter and gray matter based on fMRI for Alzheimer's disease classification *Brain Behav* **9** e01407
[19] Allioui H, Sadgal M and Elfazziki A 2019 Deep MRI segmentation: a convolutional method applied to Alzheimer's Disease detection *Int J Adv Comput Sci Appl* **10** 365–71
[20] Stern R A, Adler C H, Chen K and Navitsky M 2019 Tau positron-emission tomography in former national football league players *N. Engl. J. Med.* **380** 1716–25
[21] Prosser A M J, Tossici-Bolt L and Kipps C M 2020 The impact of regional 99mTc-HMPAO single-photon-emission computed tomography (SPECT) imaging on clinician diagnostic confidence in a mixed cognitive impairment sample *Clin Radiol* **75** 714–22
[22] De Bay D R, Reid G A, Pottie I R, Martin E, Bowen C V and Darvesh S 2017 Targeting butyrylcholinesterase for preclinical single photon emission computed tomography (SPECT) imaging of Alzheimer's Disease *Alzheimer's Dement Transl Res Clin Interv* **3** 166–76
[23] Turner R S, Stubbs T, Davies D A and Albensi B C 2020 Potential new approaches for diagnosis of Alzheimer's Disease and related dementias *Front Neurol* **11** 496–506
[24] Lermyte F, Everett J, Lam Y P, Wootton C A, Brooks J, Barrow M P, Telling N D, Sadler P J, O'connor P B and Collingwood J F 2019 Metal ion binding to the amyloid β monomer studied by native top-down FTICR mass spectrometry *J. Am. Soc. Mass. Spectrom.* **30** 2123–34
[25] Lima D, Hacke A C M, Inaba J, Pessoa C A and Kerman K 2020 Electrochemical detection of specific interactions between apolipoprotein E isoforms and DNA sequences related to Alzheimer's Disease *Bioelectrochemistry* **133** 1–9
[26] Phan L M T, Hoang T X, Vo T A T, Pam H L, Le H T N and Chinnadayyala S R 2021 Nanomaterial-based optical and electrochemical biosensors for amyloid beta and tau: potential for early diagnosis of Alzheimer's Disease *Expert Rev. Mol. Diagn.* **21** 175–93
[27] Manna M, Roy S, Bhandari S and Chattopadhyay A 2020 A dual-emitting quantum dot complex nanoprobe for ratiometric and visual detection of Hg 2^+ and Cu 2^+ ions *J. Mater. Chem. C* **8** 6972–6
[28] Chang K L and Ho P C J P O 2014 Gas chromatography time-of-flight mass spectrometry (GC-TOF-MS)-based metabolomics for comparison of caffeinated and decaffeinated coffee and its implications for Alzheimer's Disease *PLoS One* **9** e104621
[29] Kunkle B W, Grenier-Boley B and Sims R 2019 Genetic meta-analysis of diagnosed Alzheimer's Disease identifies new risk loci and implicates Aβ, tau, immunity and lipid processing *Nat. Genet.* **51** 414–30
[30] Janik M, Hamidi S V, Koba M, Perreault J, Walsh R, Bock W J and Smietane M 2021 Real-time isothermal DNA amplification monitoring in picoliter volumes using an optical fiber sensor *Lab Chip* **21** 397–404
[31] Esposito F, Sansone L, Srivastava A, Baldini F, Campopiano S, Chiavaioli F, Giordano M, Giannetti A and Iadicicoco A 2021 Long period grating in double cladding fiber coated with graphene oxide as high-performance optical platform for biosensing *Biosens Bioelectronics* **172** 112747
[32] Moro G, Chiavaioli F, Liberi S, Zubiate P, Villar I, Angelini A, Wael K D, Baldini F, Moretto L M and Giannetti A 2021 (INVITED) nanocoated fiber label-free biosensing for perfluorooctanoic acid detection by lossy mode resonance *Res Opt* **5** 100123
[33] Gagni P, Sola L, Cretich M and Chiari M 2013 Development of a high-sensitivity immunoassay for amyloid-beta 1–42 using a silicon microarray platform *Biosens. Bioelectron.* **47** 490–5
[34] Sierks M R, Chatterjee G, McGraw C, Kasturirangan S, Schulz P and Parasad S 2011 CSF levels of oligomeric alpha-synuclein and beta-amyloid as biomarkers for neurodegenerative disease *Integr. Biol.* **3** 1188–96
[35] Lee Y K, Lee K S, Kim W M and Sohn Y S 2014 Detection of amyloid-b42 using a waveguide-coupled bimetallic surface plasmon resonance sensor chip in the intensity measurement mode *PLoS One* **9** e98992
[36] Frost S *et al* 2013 Retinal vascular biomarkers for early detection and monitoring of Alzheimer's Disease *Transl Psychiatry* **3** e233
[37] Nair R V, Yi P J, Padmanabhan P, Gulyas B and Murukeshan V M 2020 Au nano-urchins enabled localized surface plasmon resonance sensing of beta amyloid fibrillation *Nanoscale Adv* **2** 2693–8
[38] Kim J, Kim S, Nguyen T T, Lee R, Li T, Yun C, Ham Y, An S S A and Ju H 2016 Label-free quantitative immunoassay of fibrinogen in Alzheimer Disease patient plasma using fiber optical surface plasmon resonance *J. Electron. Mater.* **45** 2354–60
[39] Nguyen T T, Bea S O, Kim D M, Yoon W J, Park J W, An S S A and Ju H 2105 A regenerative label-free fiber optic sensor using surface plasmon resonance for clinical diagnosis of fibrinogen *Int J Nanomedicine* **10** 155–62
[40] Kant R 2020 Surface plasmon resonance based fiber–optic nanosensor for the pesticide fenitrothion utilizing Ta2O5 nanostructures sequestered onto a reduced graphene oxide matrix *Microchim. Acta* **187** 8–19
[41] Wang C 2009 Fiber loop ringdown — a time-domain sensing technique for multi-function fiber optic sensor platforms: current status and design perspectives *Sensors* **9** 7595–621
[42] Kaya M and Wang C 2014 'Fiber loop ringdown glucose sensors: initial tests in human diabetic urines' *Proc. SPIE 9098, Fiber Optic Sensors and Applications XI, 90980O*
[43] Brown R S, Kozin I, Tong Z, Oleschuk R D and Loock H P 2002 Fiber-loop ring-down spectroscopy *J. Chem. Phys.* **117** 10444-10447
[44] Tong Z, Jakubinek M, Wright A, Gillies A and Loock H P 2003 Fiber-loop ring-down spectroscopy: a sensitive absorption technique for small liquid samples *Rev Sci Inst* **74** 4818–26
[45] Yolalmaz A, Danışman M F and Esenturk O 2019 Discrimination of chemicals via refractive index by EF-FLRD *Appl. Phys. B* **125** 1–9

[46] Chiavaioli F 2018 Detection of Alzheimer's Tau protein using nanocoated fiber biosensors *Consiglio Nazionale Delle Ricerche —Istituto Di Fisica Applicata 'Nello Carrara'* https://cnr.it/it/mobilita-breve-durata/da-cnr-a-universita-istitutizioni-ricerca-estere/relazione/2017-2037/relazione-finale-chiavaioli-signed.pdf
[47] Chiavaioli F, Zubiate P, Villar D V, Zammareno C R, Gianneti A, Tombelli S, Trono C, Arregu F J, Matias I R and Baldini F 2018 Femtomolar detection by nanocoated fiber label-free biosensors *ACS Sens.* **5** 936–43
[48] Nu T T V, Tran N H T, Nam E, Nguyen T T, Yoon W J, Cho S, Kim J, Chang K A and Ju H 2018 Blood-based immunoassay of tau proteins for early diagnosis of Alzheimer's Disease using surface plasmon resonance fiber sensors *RSC Adv.* **8** 7855–62
[49] Kant R and Gupta B D 2018 Fiber-optic SPR based acetylcholine biosensor using enzyme functionalized Ta_2O_5 nanoflakes for Alzheimer's Disease diagnosis *Lightwave Technol* **18** 4018–24
[50] Sun J J, Lee S J, Wu L, Sarntinoranont M and Xie H 2012 Refractive index measurement of acute rat brain tissue slices using optical coherence tomography *Opt. Express* **16** 1084–95
[51] Kaya M 2020 Fiber optic chemical sensors for water testing by using fiber loop ringdown spectroscopy technique *Turk J Elec Eng & Comp Sci* **28** 2375-2084
[52] Kaya M and Esenturk O 2020 Highly sensitive fiber optic pressure sensors for wind turbine applications *Turk J Elec Eng & Comp Sci* **28** 2789–96
[53] Kaya M and Esenturk O 2020 Study of strain measurement by fiber optic sensors with a sensitive fiber loop ringdown spectrometer *Opt. Fiber Technol.* **54** 102070
[54] Kaya M, Sahay P and Wang C 2013 *Sens Actuators B Chem* **176** 803–10
[55] Wang C, Kaya M and Wang C 2012 Evanescent field-fiber loop ringdown glucose sensor *J. Biomed. Opt.* **17** 037004
[56] Herath C, Wang C, Kaya M and Chevalier D 2011 Fiber loop ringdown DNA and bacteria sensors *J. Biomed. Opt.* **16** 050501
[57] Sahay P, Kaya M and Wang C 2013 Fiber loop ringdown sensor for potential real-time monitoring of cracks in concrete structures: an exploratory study *Sensors* **13** 39–57
[58] Cengiz B 2013 Fiber loop ring down spectroscopy for trace chemical detection *MS Thesis* Middle East Technical University (METU)
[59] Clowes J R, McInnes J, Zervas M N and Payne D N 1998 Effects of high temperature and pressureon silica optical fiber sensors *IEEE Photon Tech Lett* **10** 403–5
[60] Waxler R M and Cleek G W 1973 The effect of temperature and pressure on the refractive index of some oxide glasses *J Res Natl Bur Stand A Phys Chem* **77** 755–63
[61] Chiavaioli F, Gouveia C A J, Jorge P A S and Baldini F 2017 Towards a uniform metrological assessment of grating-based optical fiber sensors: from refractometers to biosensors *Biosensors* **7** 7020023
[62] Liu F, Zhang X, Li K, Guo T, Ianoul A and Albert J 2021 Discrimination of bulk and surface refractive index change in plasmonic sensors with narrow bandwidth resonance combs *ACS Sens.* **6** 3013–23
[63] Wei T, Han Y, Li Y, Tsai H L and Xiao H 2008 Temperature-insensitive miniaturized fiber inline Fabry–Perot interferometer for highly sensitive refractive index measurement *Opt. Express* **16** 5764–9
[64] Sciacca B, François A, Hoffman M K, Brazzatti J, Penno M, Hoffmann P and Monro T M 2013 Radiative-surface plasmon resonance for the detection of apolipoprotein E in medical diagnostics applications *Nanomed: Nanotechnol Biol Med* **9** 550–7